ARTICLE

Spin Gapless Semiconductor–Metal–Half-Metal Properties in Nitrogen-Doped Zigzag Graphene Nanoribbons

Yafei Li,[†] Zhen Zhou,[†,*] Panwen Shen,[†] and Zhongfang Chen[‡,*]

[†]Institute of New Energy Material Chemistry, College of Chemistry, Institute of Scientific Computing, Nankai University, Tianjin 300071, People's Republic of China, and [‡]Department of Chemistry, Institute for Functional Nanomaterials, University of Puerto Rico, Rio Piedras Campus, San Juan, Puerto Rico 00931

ABSTRACT The geometries, formation energies, and electronic and magnetic properties of N-doping defects, including single atom substitution and pyridine- and pyrrole-like substructures in zigzag graphene nanoribbons (ZGNRs), were investigated by means of spin-unrestricted density functional theory computations. The edge carbon atoms are more easily substituted with N atoms, and three-nitrogen vacancy (3NV) defect and four-nitrogen divacancy (4ND) defect also prefer the ribbon edge. Single N atom substitution and pyridine- and pyrrole-like N-doping defects can all break the degeneracy of the spin polarization of pristine ZGNRs. One single N atom substitution makes the antiferromagnetic semiconducting ZGNRs into spin gapless semiconductors, while double edge substitution transforms N-doped graphenes into metals. Pyridine- and pyrrole-like N-doping defects make ZGNRs into half-metals or spin gapless semiconductors. These results suggest the potential applications of N-doped ZGNRs in nanoelectronics.

KEYWORDS: graphene · N-doped graphene · density functional theory · electronic properties · magnetic properties · nanoelectronics

Since its experimental realization in 2004,[1,2] graphene, a single atomic layer of graphite, has shown exciting unusual properties and is bringing us revolutions to many advanced materials that we desire.[3−6] Two dimensional (2D) graphene has many advantages over other carbon nanomaterials (fullerenes and nanotubes), such as massless relativistic Dirac Fermion,[7,8] room-temperature quantized Hall effect,[9] high-speed mobility of carriers,[10,11] and the largest strength ever measured.[12] Very recently, it has been reported that graphene can react with atomic hydrogen to form the insulating derivate, graphane.[13] All these make graphene an important candidate for the future nanoelectronics.[14−16]

Following graphene, one-dimensional (1D) graphene nanoribbons (GNRs) have also been realized experimentally by cutting graphene in nanometer-sized width.[1] Due to the excellent geometrics, GNRs can be conveniently designed into various devices. The electronic and magnetic properties of graphene nanoribbons have been intensively studied theoretically.[17−32] Son *et al.*[24] demonstrated that H-terminated GNRs with either armchair or zigzag shaped edges have a nonzero energy gap, which has been confirmed experimentally by Li *et al.*[33] and Riter *et al.*[34] very recently. Especially, Ritter and Lyding[34] demonstrated that GNRs with a higher fraction of zigzag edges exhibit a smaller energy gap than a predominantly armchair edge ribbon of similar width.

The zigzag graphene nanoribbons (ZGNRs) have special localized edge states, which are antiferromagnetically coupled to each other.[17,18,24] Interestingly, under an external transverse electronic field,[31] the degeneracy of the edge states is broken and the intriguing half-metallicity (the coexistence of metallic nature for electrons with one spin orientation and insulating nature for electrons with the other) can be realized in zigzag GNRs. Hod *et al.*[28] reported that edge oxidation can make the ribbons more stable and lower the onset electron field required to induce half-metallic behavior. Kan *et al.*[32] showed that without external electron field zigzag GNRs with $-NO_2$ groups at one edge and $-CH_3$ groups at the other could also be half-metals. The aforementioned studies hold the promising applications in nanoelectronics.

Doping with foreign atoms, such as B and N, has proven to be an effective way to tune the electronic properties of carbon nanotubes and widen their applications.[35−45] Nitrogen doping brings a carrier, while B doping gives birth to a hole, which could turn carbon nanotubes into n-

*Address correspondence to zhouzhen@nankai.edu.cn, zhongfangchen@gmail.com.

Received for review April 4, 2009 and accepted June 19, 2009.

Published online June 25, 2009. 10.1021/nn9003428 CCC: $40.75

and p-type semiconductors, respectively. Doping is also feasible to modify the electronic properties of GNRs.[46−53] Martins *et al.* reported that B[46] and N[47] doping at the edges of ZGNRs results in distinct charge transport properties for each spin channel of GNRs; therefore, the doped GNRs can be used as spin filter devices. Yu *et al.*[48] studied the effect of N doping on the electronic properties of zigzag GNRs and found that the electronic properties of N-doped GNRs are dependent on the doping site. Several groups found that the doping can lead to a metal−semiconductor transition.[46−50] However, some issues have not been clearly resolved, for example, the effects of N doping on the magnetic properties of GNRs are not involved and also the substitution concentration effect has not been investigated.

Besides single atom substitution as mentioned above, some special doping defects, such as pyridine-like substructures, can also form in graphene nanoribbons. The effects of pyridine-like substructures have well been studied on the electronic structures of carbon nanotubes.[42,54,55] There are two kinds of pyridine-like substructures, namely, three-nitrogen vacancy (3NV) and four-nitrogen divacancy (4ND). In most previous studies,[42,54] a pyridine-like structure was referred to as 3NV defect, where nitrogen atoms are substituted for three carbon atoms neighboring the vacancy. Very recently, Rocha *et al.*[56] suggested that the 4ND defect is actually more stable in carbon nanotubes, which was also confirmed by our recent theoretical study.[55] However, the relative stability of 3NV and 4ND defects in GNRs is still an open question. Cervantes-Sodi *et al.*[49] reported that 3NV defects in armchair GNRs could induce a semiconductor−metal transition. However, pyridine-like N-doping defects in zigzag GNRs have not been studied to our best knowledge.

Not only the above inspiring theoretical findings but also the very recent experimental achievements are exciting. Wei *et al.*[57] synthesized N-doped graphene, the first experimental example of the substitutionally doped graphene, by a chemical vapor deposition method. Three types of N atoms were simultaneously identified in the N-doped graphene, namely, the "graphitic" (single N atom substitution), "pyridinic" (pyridine-like), and "pyrrolic" (pyrrole-like) nitrogen, among which the graphitic nitrogen dominates. They also found that the N-doped graphene exhibits n-type semiconductor behavior, consistent with previous theoretical prediction.[46,50] Quite recently, Wang *et al.*[58] reported that *via* high-power electrical joule heating in ammonia gas C−N bonds form at the high reactive edges of GNRs, resulting in n-type semiconductors.

In this work, we carried out density functional theory (DFT) computations to investigate the effects of N-doping defects, including single N atom substitution, pyridine- and pyrrole-like N substructures, on the geometries, formation energies, and the electronic and magnetic properties of ZGNRs. Several findings are especially intriguing: the recently proposed spin gapless semiconductor (SGS)[59] can be realized in ZGNRs by single edge substitution; double edge substitution can transform ZGNRs into metals; pyridine- and pyrrole-like substructures make ZGNRs into half-metals or SGSs. These findings suggest the potential applications of N-doped ZGNRs to spintronics.

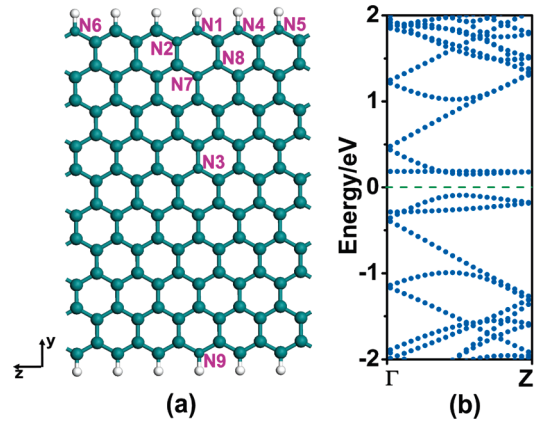

Figure 1. (a) Structural model of 10-ZGNR. The ribbon is assumed to be infinite along the *z* direction. Carbon and hydrogen atoms are denoted with gray and white balls, respectively. The N doping sites are also indicated with shrunken balls. (b) Antiferromagnetic band structure of 10-ZGNR. The dashed line denotes the position of Fermi level.

RESULTS AND DISCUSSION

10-ZGNR. Following the previous convention,[17−20] we define the width parameter N_z of zigzag graphene nanoribbons as the number of zigzag lines across the ribbon width, as exemplified by 10-ZGNR (Figure 1a). The edge carbon atoms of the nanoribbon are all saturated with H atoms to avoid the dangling bond states. Several sites for single N substitutions were considered (N1−N9 in Figure 1).

First, we computed the total energies for different magnetic phases of 10-ZGNR, including nonmagnetic (NM), ferromagnetic (FM), and antiferromagnetic (AFM) ones, to determine the ground state. The total energy of the FM phase is 8.5 meV/unit lower than that of the NM phase but 0.2 meV/unit higher than that of the AFM phase. Therefore, energetically, the AFM phase is the most favorable for 10-ZGNR. The magnetization per edge atom for each spin on each sublattice of the AFM phase is 0.19 μ_B with opposite orientations, and the net magnetic moment of the system is zero. Figure 1b presents spin-resolved band structures of pristine 10-ZGNR. The spin-up and spin-down bands are fully degenerate, and a 0.27 eV energy gap is opened between spin-polarized π and π^* bands, which are quite flat near the Fermi level. Our results achieve good agreement with previous studies,[24,25,31] indicating that the methodology adopted in this work can give a reliable description of electronic and magnetic properties of ZGNRs.

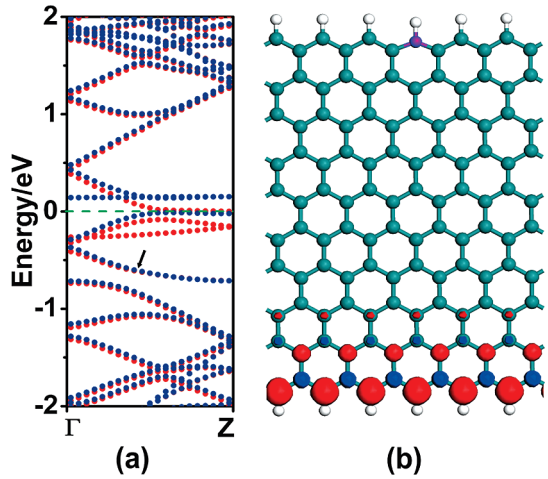

Figure 2. (a) Band structure for N1 configuration. The blue and red dots denote spin-up and spin-down channels, respectively. (b) Ground state spatial distribution of charge difference between spin-up and spin-down channels for N1 configuration. The N atom is denoted with a purple ball. The isovalues for the blue and red isosurfaces are 0.01 and −0.01 e/Å^3, respectively.

One N Atom Substitution in 10-ZGNR. We considered several configurations for 10-ZGNR containing a substitutional N atom, such as N1, N2, and N3 configurations, as denoted in Figure 1a. Our computations show that the N doping at the edge of 10-ZGNR (N1) is energetically the most favorable. For N1 configuration, the substitution leads to a slight local deformation. The lengths of C−N and N−H bonds are 1.38 and 1.02 Å, respectively, slightly shorter than the edge C−C and C−H bonds (1.41 and 1.09 Å, respectively). The formation energy of N1 configuration is exothermic (−0.63 eV). However, for N2 and N3 configurations, the formation energies are endothermic (0.48 and 0.77 eV, respectively). Thus, the carbon atoms close to the edges are more likely to be substituted than those in the interior sites (such as N2 and N3), which can be attributed to the decay of edge states. Similar results were reported previously.[48]

In Figure 2a, we show the spin-resolved band structure of the most stable configuration N1. Compared with pristine 10-ZGNR (Figure 1b), N1 configuration presents asymmetrical spin-up and spin-down bands, which means that the spin degeneracy has been broken. Moreover, one spin-polarized band below the Fermi level in the spin-up channel and one spin-polarized band above the Fermi level in the spin-down channel are both removed. Each spin channel shows semiconducting characteristics; the band gaps are 0.18 and 0.10 eV for spin-up and spin-down channels, respectively, which are lower than pristine 10-ZGNR. Besides the perturbation to the edge bands, N doping also brings impurity states in both spin-up and spin-down channels below the Fermi level (marked with an arrow). Note that the impurity states in two spin bands are almost degenerate.

Interestingly, as can be seen in Figure 2a, the conduction band minimum (CBM) of the spin-up channel and the valence band maximum (VBM) in the spin-down channel touch each other at the Fermi level, and the band gap is therefore closed. It implies that N1 configuration is a typical spin gapless semiconductor (SGS) (or a semimetal with a vanishing density of states), proposed by Wang very recently.[53] For N1 configuration, no energy is required to excite the electrons from the valence band to the conduction band, and the excited electrons can achieve 100% spin polarization at the Fermi level, like half-metals. Spin gapless semiconductors are quite promising candidates for spin devices. To test the dependence of the "spin gapless" property on the ribbon width, we have computed the band structures of several ribbons in addition to 10-ZGNR. The results (see Figure S1 in Supporting Information) show that they are all SGSs. The traditional methods used to design SGSs usually accompany with toxic gapless semiconductors and doped transition metals. However, our study proposes a flexible way of designing metal-free SGSs though N doping at the edge of zigzag GNRs. To our best knowledge, this is the first report of SGSs based on GNRs.

To clarify the origin of the broken spin degeneracy, we computed the ground state spatial spin distribution of N1 configuration. When one N atom is introduced to the edge of 10-ZGNR (Figure 2a), the spin polarization on the doped edge (upper) is completely suppressed, and there is no unpaired spin localized on the N atom, which can explain why the impurity states are nearly degenerate. In contrast, the spin polarization on the undoped edge (lower) is less influenced, and the magnetization per edge atom is still 0.19 μ_B, which is equal to that of pristine 10-ZGNR. The net magnetic moment of N1 configuration is 0.95 μ_B. Moreover, we found that one substitutional N atom at the N2 site (N2 configuration) can also lead to the suppression of spin polarization (see Figure S2 in Supporting Information). Huang *et al.*[50] have recently reported that vacancies and B doping at the edge of zigzag GNRs have the same effect. Thus, the heteroatom doping is indubitably responsible for the breaking of spin degeneracy.

Two Substitutional N Atoms in 10-ZGNR. We examined several possible N−N configurations, as indicated in Fig-

TABLE 1. N−N Distance and Formation Energy per N Atom for Two Substitutional N Atoms in 10-ZGNR (See Text for the Definition of Formation Energy)

configuration	N1−N2	N1−N4	N1−N5	N1−N6	N1−N7	N1−N8	N1−N9
N−N distance (Å)	1.39	2.38	4.33	7.88	2.78	2.38	19.78
formation energy (eV)	0.65	0.08	−0.42	−0.53	−0.04	0.10	−0.63

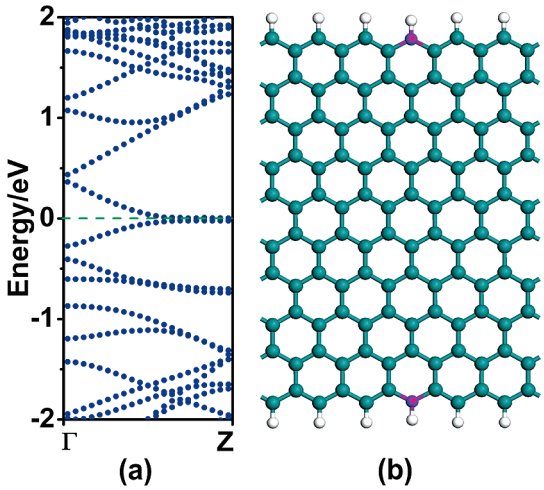

Figure 3. (a) Electronic band structure of the N1−N9 configuration. (b) Ground state spatial spin distribution of the N1−N9 configuration.

ure 1a, including N1−N2, N1−N4, N1−N5, N1−N6, N1−N7, N1−N8, and N1−N9. Table 1 shows the formation energies of two substitutional N atoms and optimized N−N distances in 10-ZGNRs for various configurations. The N1−N9 configuration, in which two N atoms are localized in the opposite edges, has the lowest formation energy (−0.63 eV/N) and is the most favorable energetically. This formation energy per N atom is equal to that of the N1 configuration. The N1−N2 configuration, in which two N atoms are the nearest neighbors, has the highest formation energy (0.65 eV/N). The same trend was reported by Martins *et al.* for two doped B atoms in graphene nanoribbons.[46]

Figure 3 presents the electronic band structure for the N1−N9 configuration. The spin-up and spin-down channels are both fully degenerate, and the lowest conduction band and the highest valence band touch at the Fermi level; hence, this N-doped nanoribbon becomes metallic. Similar band structures were found for other zigzag nanoribbons (see Figure S3 in Supporting Information). To study the magnetic properties, we have also computed the spin distribution of the N1−N9 configuration at the ground state. As shown in Figure 3b, the spin polarizations on two edges are both suppressed and the net magnetic moment of the supercell is zero, which means that 10-ZGNR becomes nonmagnetic.

Defects with Pyridine- or Pyrrole-like Subunit. One special N-doping defect, pyridine-like structure, usually exists in graphene-based systems. Here, three types of pyridine-like structures are considered: 3NV defect, 4ND defect, and pyridine-like N atom on the edge (Figure 4). A 3NV defect in 10-ZGNR can be constructed by removing a C atom and substituting the three nearest neighbor C atoms with N atoms (see Figure 4a), while a 4ND defect can be constructed by deleting a C−C bond and substituting the four nearest neighbor C atoms with N atoms (see Figure 4b). The edge pyridine-like N atom is constructed by substituting one C−H with a N atom. For 3NV and 4ND defects, we have considered many possible configurations since the defect can exist in different sites of ZGNR (see Figure S4 in Supporting Information). Our computations show that the configuration with defects close to the edge is favorable energetically. The schematic representations for the most stable configurations of 10-ZGNR containing a pyridine-like N-doping defect are shown in Figure 4a−c. The formation energy for 10-ZGNR containing a 3NV defect is 2.73 eV, which is 0.87 eV lower than that of 4ND defect. Therefore, the 3NV defect is more likely to form in 10-ZGNR than the 4ND defect. Note that 4ND is more preferred in carbon nanotubes,[55,56] which is due to the fact that a divacancy is more favorable for nanotubes to release surface strain than a single vacancy.

The formation energy for the edge pyridine-like N atom (see Figure 4c) is 0.48 eV, which is higher than that of substitutional N atom (−0.63 eV) due to the removal of H atom. Moreover, we have also considered the case of 10-ZGNR containing a pyrrole-like N-doping defect (see Figure 4d). Following the proposal of ref 51, the pyrrole-like N atom is constructed by deleting a C−C bond and substituting the two nearest neighbor

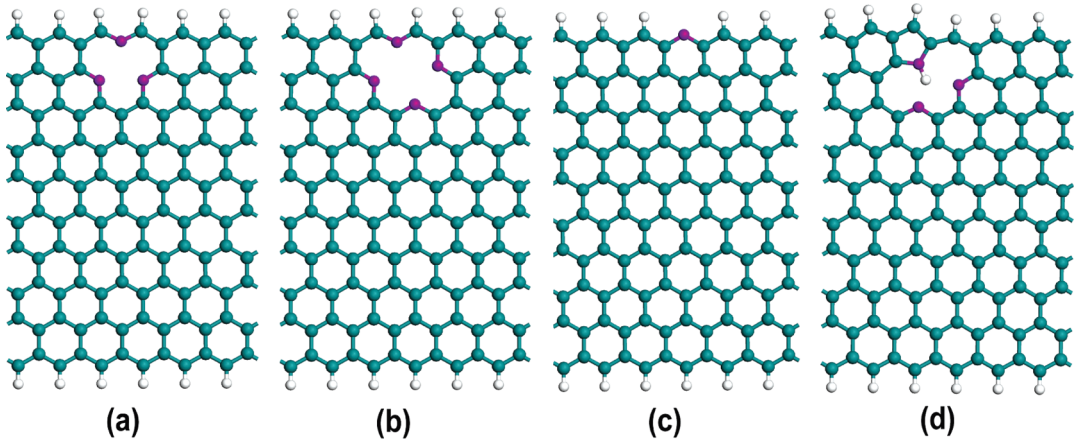

Figure 4. Schematic representations for 10-ZGNR containing a 3NV (a), 4ND (b), edge pyridine-like N atom (c), and pyrrole-like N-doping defect (d).

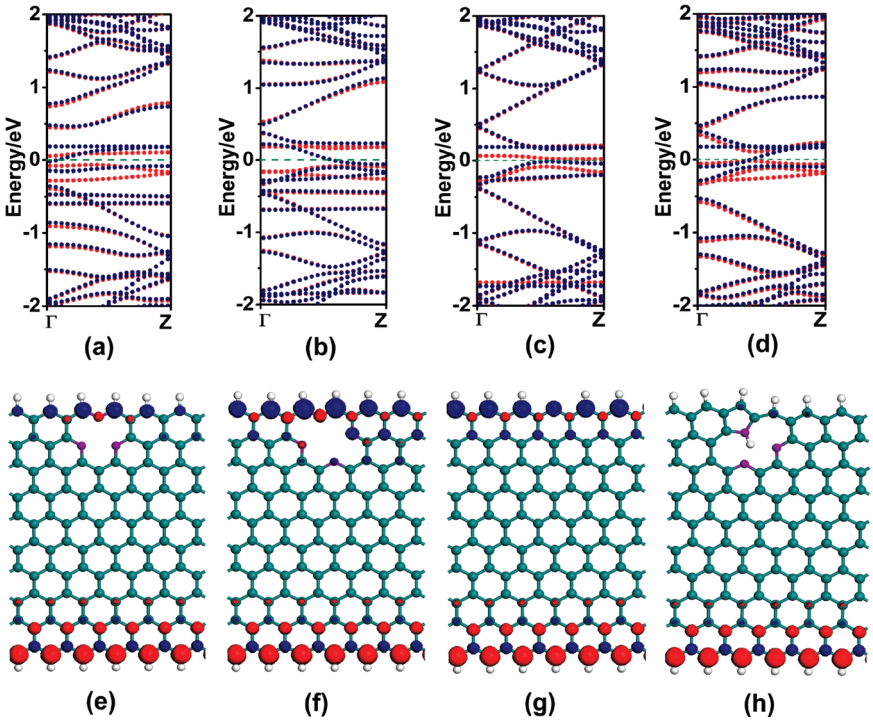

Figure 5. Band structures and isosurfaces of charge difference between spin-up and spin-down channels for 10-ZGNR containing a 3NV (a,e), 4ND (b,f), edge pyridine-like N atom (c,g), and pyrrole-like N doping (d,h) defect.

C atoms with N atoms, the left two nearest neighbor C atoms are substituted by N−H to form a five-membered ring. Pyrrole-like N-doping defect in 10-ZGNR also prefers to be localized near the ribbon edge and introduces remarkable geometry deformation to the ribbon edge. The formation energy for 10-ZGNR containing a pyrrole-like N-doping defect is 2.96 eV, which is lower than those of 3NV and 4ND defects.

The pyridine- or pyrrole-like N-doping defects bring remarkable changes into the band structure of 10-ZGNR (Figure 5). After the introduction of a 3NV defect, the energy bands near the Fermi level become asymmetric for different spin channels: in the spin-up channel, the Fermi level is shifted into the conduction band and the metallicity is thus obtained, while the spin-down channel is semiconducting with a 0.12 eV gap. Therefore, the 10-ZGNR containing a 3NV defect is half-metallic. Similarly, the 10-ZGNR containing a 4ND defect is also half-metallic, with a metallic spin-down channel and a 0.38 eV gap for the spin-up channel. The introduction of 3NV and 4ND defects gives many impurity states in both conduction and valence bands. When a pyridine-like N atom appears at the edge of 10-ZGNR, both spin channels show semiconducting characteristics with 0.19 and 0.10 eV band gap for spin-up and spin-down channels, respectively. Especially, the CBM of the spin-up channel and the VBM in the spin-down channel touch each other at the Fermi level. Therefore, similar to N1 configuration, 10-ZGNR containing an edge pyridine-like N atom is also a SGS. For 10-ZGNR containing a pyrrole-like N-doping defect, the energy bands close to the Fermi level show a metallic spin-up channel and a semiconducting spin-down channel with a 0.13 eV band gap, thus the half-metallic behavior is obtained. The above results demonstrate that the introduction of pyridine- and pyrrole-like subunits in zigzag GNRs can also lead to the breaking of spin degeneracy, suggesting a feasible way of building spin devices based on GNRs.

The pyridine- or pyrrole-like N-doping defects also have significant effects on the spin distributions of the defective 10-ZGNRs (Figure 5). For those pyridine-like defects in 10-ZGNRs, the unpaired spins are mainly concentrated on two edges. The net magnetic moments for 10-ZGNR containing a 3NV, 4ND, and edge pyridine-like N-doping defect are 0.67, 0.22, and 0.32 μ_B, respectively. Unlike the case of single N atom doping, although there is a substitutional N atom localized on the edge site for pyridine-like defects, the spins on the edges close to the defects are not removed. Especially, some unpaired spins are localized on pyridine-like N atoms. The above results should be attributed to the non-doping feature of pyridine-like N atom.[60] The N atom has five valence electrons, pyridine-like N atom uses two of its electrons to form two σ bonds with carbon atoms, and the rest of the three electrons are used to form one π state and one lone pair. Therefore, pyridine-like defects in GNRs have less influence on the spin polarization of the edge states than single substitutional N atoms. In contrast, when a pyrrole-like N-doping defect appears at the edge of 10-ZGNR, the spin polarization on the doped edge is nearly removed and a net magnetic moment of 0.95 μ_B appears, which is quite similar to that single N atom substitution. Both pyrrole-like and substitutional N atoms use three electrons to form σ bonds and use the left two electrons to form a π state and a π^* state. Therefore, they affect the edge states significantly and are characterized as π-doping defects.

In summary, the effects of N-doping defects, including single atom substitution and pyridine- and pyrrole-like substructures on the energetics, electronic, and magnetic properties of ZGNRs, have been studied through spin-unrestricted density functional theory computations. When one subtitutional N atom is introduced into the bonding networks of ZGNRs, it energetically prefers to be localized at the ribbon edge. One N doping can remove the spin polarization of the doped edge and make ZGNRs spin gapless semiconductors. When the second N atom is substituted for carbon atom,

two N atoms are preferably localized at two opposite edges and make ZGNRs nonmagnetic metals. The pyridine- and pyrrole-like structures, in which the vacancies are present, also prefer to form near the ribbon edges. The degeneracy of the two edge states is broken due to the presence of defects, and the doped ZGNRs are spin gapless semiconductors or half-metals. Our computations point out a feasible way for achieving spintronics devices based on ZGNRs. The successful synthesis of N-doped graphenes[57] and the progress in controlling formation of graphene nanoribbons[61] make us rather confident in obtaining the well-defined N-doped ZGNRs and realizing their novel intrinsic electronic and magnetic properties in the nanodevices in the very near future.

COMPUTATIONAL METHODS

Our spin-unrestricted DFT computations employed an all-electron method within a generalized gradient approximation (GGA) for the exchange-correlation term, as implemented in the DMol^3 code.[62] The double numerical plus polarization (DNP) basis set and PW91 functional[63] were adopted in all the computations. Self-consistent field (SCF) calculations were carried out with a convergence criterion of 10^{-6} au on the total energy and the electron density. To ensure high-quality computational results, the real-space global orbital cutoff radius was chosen to be as high as 5.5 Å. Three Monkhorst−Pack k points were used for geometry optimization to sample the 1D Brillouin zone, and the band structures were computed with 21 k points based on the optimized structures. One-dimensional periodic boundary condition (PBC) was applied along the ribbon axis. Our supercell model includes six units, and the supercell is large enough to ensure that the vacuum space is at least 12 Å. No changes were found for the total energy when the vacuum was further increased.

The formation energy E_f of single atom substitution, 3NV, and 4ND defect is defined as $E_f = (E_N + n_C\mu_C) - (E_P + n_N\mu_N)$, where E_P and E_N are the total energies of pristine and N-doped GNRs, respectively; n_C and n_N are the number of removed C and doped N atoms, respectively; μ_C is the cohesive energy of infinite graphene, and μ_N is taken as the half of the binding energy of N_2. For edge pyridine-like N atom and pyrrole-like N-doping defect, the formation energies are computed using the equation, $E_f = (E_N + \mu_C + \mu_H) - (E_P + \mu_N)$ and $E_f = (E_N + 4\ \mu_C) - (E_P + 3\ \mu_N + \mu_H)$, respectively; μ_H is taken as the half of the binding energies of H_2. Thus, the system is energetically more favorable when the formation energy is lower.

Acknowledgment. Support in China by NSFC (20873067) and NCET, and in the USA by NSF Grant CHE-0716718, the Institute for Functional Nanomaterials (NSF Grant 0701525), and U.S. Environmental Protection Agency (EPA Grant No. RD-83385601) is gratefully acknowledged.

Supporting Information Available: Band structures for other ZGNRs containing one or two substitutional N atoms, distributions of unpaired spins of 10-ZGNR with one subtitutional N atom at the N2 site, and optimized configurations and corresponding formation energies for 10-ZGNR containing 3NV, 4ND, or pyrrole-like N-doping defect. This material is available free of charge *via* the Internet at http://pubs.acs.org.

REFERENCES AND NOTES

1. Novoselov, K. S.; Geim, A. K.; Morozov, S. V.; Jiang, D.; Zhang, Y.; Dubonos, S. V.; Gregorieva, I. V.; Firsov, A. A. Electric Field Effect in Atomically Thin Carbon Films. *Science* **2004**, *306*, 666–669.
2. Novoselov, K. S.; Jiang, D.; Schedin, F.; Booth, T. J.; Khotkevich, V. V.; Morozov, S. V.; Geim, A. K. Two-Dimensional Atomic Crystals. *Proc. Natl. Acad. Sci. U.S.A.* **2005**, *102*, 10451–10453.
3. Li, D.; Kaner, R. B. Graphene-Based Materials. *Science* **2008**, *320*, 1170–1171.
4. Rogers, J. A. Making Graphene for Macroelectronics. *Nat. Nanotechnol.* **2008**, *3*, 254–255.
5. Brumfiel, G. Graphene Gets Ready for the Big Time. *Nature* **2009**, *458*, 390–391.
6. Service, R. F. Carbon Sheets an Atom Thick Give Rise to Graphene Dreams. *Science* **2009**, *324*, 875–877.
7. Katsnelson, M. I.; Novoselov, K. S.; Geim, A. K. Chiral Tunnelling and the Klein Paradox in Graphene. *Nat. Phys.* **2006**, *2*, 620–625.
8. Katsnelson, M. I.; Novoselov, K. S. Graphene: New Bridge between Condensed Matter Physics and Quantum Electrodynamics. *Solid State Commun.* **2007**, *143*, 3–13.
9. Novoselov, K. S; Jiang, Z.; Zhang, Y.; Morozov, S. V.; Stormer, H. L.; Zeitler, U.; Maan, J. C.; Boebinger, G. S.; Kim, P.; Geim, A. K. Room-Temperature Quantum Hall Effect in Graphene. *Science* **2007**, *315*, 1379.
10. Zhang, Y.; Tan, Y.-W.; Stormer, H. L.; Kim, P. Experimental Observation of the Quantum Hall Effect and Berry's Phase in Graphene. *Nature* **2005**, *438*, 201–204.
11. Morozov, S. V.; Novoselov, K. S.; Katsnelson, M. I.; Schedin, F.; Elias, D.; Jaszczak, J. A.; Geim, A. K. Giant Intrinsic Carrier Mobilities in Graphene and Its Bilayer. *Phys. Rev. Lett.* **2008**, *100*, 016602.
12. Lee, C. G.; Wei, X. D.; Kysar, J. W.; Hone, J. Measurement of the Elastic Properties and Intrinsic Strength of Monolayer Graphene. *Science* **2008**, *321*, 385–388.
13. Elias, D. C.; Nair, R. R.; Mohiuddin, T. M. G.; Morozov, S. V.; Blake, P.; Halsall, M. P.; Ferrairi, A. C.; Boukhvalov, D. W.; Katsnelson, M. I.; Geim, A. K. Control of Graphene's Properties by Reversible Hydrogenation: Evidence for Graphane. *Science* **2009**, *323*, 610–613.
14. Scheldin, F.; Geim, A. K.; Morozov, S. V.; Hill, E. W.; Blake, P.; Katsnelson, M. I.; Novoselov, K. S. Detection of Individual Gas Molecules Adsorbed on Graphene. *Nat. Mater.* **2007**, *6*, 652–655.
15. Geim, A. K.; Novoselov, K. S. The Rise of Graphene. *Nat. Mater.* **2007**, *6*, 183–191.
16. Zhang, Y.; Small, J. P.; Pontius, W. V.; Kim, P. Fabrication and Electric-Field-Dependent Transport Measurements of Mesoscopic Graphite Devices. *Appl. Phys. Lett.* **2005**, *86*, 073104.
17. Fujita, M.; Wakabayashi, K.; Nakada, K.; Kusakabe, K. Peculiar Localized State at Zigzag Graphite Edge. *J. Phys. Soc. Jpn.* **1996**, *65*, 1920–1923.
18. Nakada, K.; Fujita, M.; Dresselhaus, G.; Dresselhaus, M. S. Edge State in Graphene Ribbons: Nanometer Size Effect and Edge Shape Dependence. *Phys. Rev. B* **1996**, *54*, 17954–17961.
19. Wakabayashi, K.; Sigrist, M.; Fujita, M. Spin Wave Mode of Edge-Localized Magnetic States in Nanographite Zigzag Ribbons. *J. Phys. Soc. Jpn.* **1998**, *67*, 2089–2093.
20. Wakabayashi, K.; Fujita, M.; Ajiki, H.; Sigrist, M. Electronic and Magnetic Properties of Nanographite Ribbons. *Phys. Rev. B* **1999**, *59*, 8271–8282.
21. Kawai, T.; Miyamoto, Y.; Sugino, O.; Koga, Y. Graphitic Ribbons without Hydrogen-Termination: Electronic Structures and Stabilities. *Phys. Rev. B* **2000**, *62*, R116349–R116352.
22. Kusakabe, K.; Maruyama, M. Magnetic Nanographite. *Phys. Rev. B* **2003**, *67*, 092406.
23. Yamashiro, A.; Shimoi, Y.; Harigaya, K.; Wakabayashi, K. Spin- and Charge-Polarized States in Nanographene Ribbons with Zigzag Edges. *Phys. Rev. B* **2003**, *68*, 193410.
24. Son, Y.-W.; Cohen, M. L.; Louie, S. G. Energy Gaps in Graphene Nanoribbons. *Phys. Rev. Lett.* **2006**, *97*, 216803.

25. Jiang, D. E.; Sumpter, B. G.; Dai, S. First Principles Study of Magnetism in Nanographenes. *J. Chem. Phys.* **2007**, *127*, 124703.
26. Jiang, D. E.; Sumpter, B. G.; Dai, S. Unique Chemical Reactivity of a Graphene Nanoribbon's Zigzag Edge. *J. Chem. Phys.* **2007**, *126*, 134701.
27. Barone, V.; Hod, O.; Scuseria, G. E. Electronic Structure and Stability of Semiconducting Graphene Nanoribbons. *Nano Lett.* **2006**, *6*, 2748–2754.
28. Hod, O.; Barone, V.; Peralta, J. E.; Scuseria, G. E. Enhanced Half-Metallicity in Edge-Oxidized Zigzag Graphene Nanoribbons. *Nano Lett.* **2007**, *7*, 2295–2299.
29. Yang, L.; Park, C. H.; Son, Y. W.; Cohen, M. L.; Louie, S. G. Quasiparticle Energies and Band Gaps in Graphene Nanoribbons. *Phys. Rev. Lett.* **2007**, *99*, 186801.
30. Han, M. Y.; Özyilmaz, B.; Zhang, Y.; Kim, P. Energy Band-Gap Engineering of Graphene Nanoribbons. *Phys. Rev. Lett.* **2007**, *98*, 206805.
31. Son, Y.-W.; Cohen, M. L.; Louie, S. G. Half-Metallic Graphene Nanoribbons. *Nature* **2006**, *444*, 347–349.
32. Kan, E. J.; Li, Z. Y.; Yang, J. L.; Hou, J. G. Half-Metallicity in Edge-Modified Zigzag Graphene Nanoribbons. *J. Am. Chem. Soc.* **2008**, *130*, 4224–4225.
33. Li, X. L.; Wang, X. R.; Zhang, L.; Lee, S. W.; Dai, H. J. Chemically Derived, Ultrasmooth Graphene Nanoribbon Semiconductors. *Science* **2008**, *319*, 1229–1232.
34. Ritter, K. A.; Lyding, J. W. The Influence of Edge Structure on the Electronic Properties of Graphene Quantum Dots and Nanoribbons. *Nat. Mater.* **2009**, *8*, 235–242.
35. Carrol, D. L.; Redlich, Ph.; Blase, X.; Charlier, J.-C.; Curran, S.; Ajayan, P. M.; Roth, S.; Rühle, M. Effects of Nanodomain Formation on the Electronic Structure of Doped Carbon Nanotubes. *Phys. Rev. Lett.* **1997**, *81*, 2332–2335.
36. Choi, H. J.; Ihm, J.; Louie, S. G.; Cohen, M. L. Defects, Quasibound States, and Quantum Conductance in Metallic Carbon Nanotubes. *Phys. Rev. Lett.* **1999**, *84*, 2917–2920.
37. Kang, H. S.; Jeong, S. Nitrogen Doping and Chirality of Carbon Nanotubes. *Phys. Rev. B* **2004**, *70*, 233411.
38. Zhou, Z.; Gao, X. P.; Yan, J.; Song, D. Y.; Morinaga, M. A First-Principles Study of Lithium Absorption in Boron- or Nitrogen-Doped Single-Walled Carbon Nanotubes. *Carbon* **2004**, *42*, 2677–2682.
39. Zhou, Z.; Gao, X. P.; Yan, J.; Song, D. Y.; Morinaga, M. Enhanced Lithium Absorption in SWCNT by Boron Doping. *J. Phys. Chem. B* **2004**, *109*, 9023–9026.
40. Zhou, Z.; Gao, X. P.; Yan, J.; Song, D. Y. Doping Effects of B and N on Hydrogen Adsorption in Single-Walled Carbon Nanotubes through Density Functional Calculations. *Carbon* **2006**, *44*, 939–947.
41. Sun, C. L.; Wang, H. W.; Hayashi, M.; Chen, L. C.; Chen, K. H. Atomic-Scale Deformation in N-Doped Carbon Nanotubes. *J. Am. Chem. Soc.* **2008**, *128*, 8368–8369.
42. Lim, S. H.; Li, R. J.; Ji, W.; Lin, J. Y. Effects of Nitrogenation on Single-Walled Carbon Nanotubes within Density Functional Theory. *Phys. Rev. B* **2007**, *76*, 195406.
43. Yu, S. S.; Wen, Q. B.; Zheng, W. T.; Jiang, Q. Effects of Doping Nitrogen Atoms on the Structure and Electronic Properties of Zigzag Single-Walled Carbon Nanotubes through First-Principles Calculations. *Nanotechnology* **2007**, *18*, 165702.
44. Koretsune, T.; Saito, S. Electronic Structure of Boron-Doped Carbon Nanotubes. *Phys. Rev. B* **2008**, *77*, 165417.
45. Bai, L.; Zhou, Z. Computational Study of B and N Doped Single-Walled Carbon Nanotubes as NH_3 and NO_2 Sensors. *Carbon* **2007**, *45*, 2105–2110.
46. Martins, T. B.; Miwa, R. H.; da Silva, A. J. R.; Fazzio, A. Electronic and Transport Properties of Boron-Doped Graphene Nanoribbons. *Phys. Rev. Lett.* **2007**, *98*, 196803.
47. Martins, T. B.; da Silva, A. J. R.; Miwa, R. H.; Fazzio, A. σ- and π-Defects at Graphene Nanoribbon Edges: Building Spin Filters. *Nano Lett.* **2008**, *8*, 2293–2298.
48. Yu, S. S.; Wen, Q. B.; Zheng, W. T.; Jiang, Q. First Principle Calculations of the Electronic Properties of Nitrogen-Doped Carbon Nanoribbons with Zigzag Edges. *Carbon* **2008**, *46*, 537–543.
49. Cervantes-Sodi, F.; Csányi, G.; Piscanec, S.; Ferrari, A. C. Edge-Functionalized and Substitutionally Doped Graphene Nanoribbons: Electronic and Spin Properties. *Phys. Rev. B* **2008**, *77*, 165427.
50. Deifallah, M.; McMillan, P. F.; Cora, F. Electronic and Structural Properties of Two-Dimensional Carbon Nitride Graphenes. *J. Phys. Chem. C* **2008**, *112*, 5447–5453.
51. Kan, E. J.; Wu, X. J.; Li, Z. Y.; Zeng, X. C.; Yang, J. L.; Hou, J. G. Half-Metallicity in Hybrid BCN Nanoribbons. *J. Chem. Phys.* **2008**, *129*, 084712.
52. Dutta, S.; Pati, S. K. Half-Metallicity in Undoped and Boron Doped Graphene Nanoribbons in the Presence of Semilocal Exchange-Correlation Interactions. *J. Phys. Chem. B* **2008**, *112*, 1333–1335.
53. Huang, B.; Liu, F.; Wu, J.; Gu, B. L.; Duan, W. H. Suppression of Spin Polarization in Graphene Nanoribbons by Edge Defects and Impurities. *Phys. Rev. B* **2008**, *77*, 153411.
54. Czrew, R.; Torrones, M.; Charlier, J.-C.; Blase, X.; Foley, B.; Kamalakaran, R.; Grobert, N.; Torrone, H.; Tekleab, D.; Ajayan, P. M.; et al. Identification of Electron Donor States in N-Doped Carbon Nanotubes. *Nano Lett.* **2001**, *1*, 457–460.
55. Li, Y. F.; Zhou, Z.; Wang, L. B. CN_x Nanotubes with Pyridinelike Structures: p-Type Semiconductors and Li Storage Materials. *J. Chem. Phys.* **2008**, *129*, 104703.
56. Rocha, R. A.; Rossi, M.; Fazzio, A.; da Silva, A. J. R. Designing Real Nanotube-Based Gas Sensors. *Phys. Rev. Lett.* **2008**, *100*, 176803.
57. Wei, D.; Liu, Y.; Wang, Y.; Zhang, H.; Huang, L.; Yu, G. Synthesis of N-Doped Graphene by Chemical Vapor Deposition and Its Electrical Properties. *Nano Lett.* **2009**, *9*, 1752–1758.
58. Wang, X.; Li, X.; Zhang, L.; Yoon, Y.; Weber, P. K.; Wang, H.; Guo, J.; Dai, H. N-Doping of Graphene Through Electrothermal Reactions with Ammonia. *Science* **2009**, *324*, 768–771.
59. Wang, X. L. Proposal for a New Class of Materials: Spin Gapless Semiconductors. *Phys. Rev. Lett.* **2008**, *100*, 156404.
60. Yang, S. H.; Shin, W. H.; Kang, J. K. The Nature of Graphite- and Pyridinelike Nitrogen Configurations in Carbon Nitride Nanotubes: Dependence on Diameter and Helicity. *Small* **2008**, *4*, 437–441.
61. Jia, X.; Hofmann, M.; Meunier, V.; Sumpter, B. G.; Campos-Delgado, J.; Romo-Herrera, J. M.; Son, H.; Hsieh, Y. P.; Reina, A.; Kong, J.; et al. Controlled Formation of Sharp Zigzag and Armchair Edges in Graphitic Nanoribbons. *Science* **2009**, *323*, 1701–1705.
62. Delley, B. An All-Electron Numerical Method for Solving the Local Density Functional for Polyatomic Molecules. *J. Chem. Phys.* **1990**, *92*, 508–517. From Molecules to Solids with the $DMol^3$ Approach. *J. Chem. Phys.* **2000**, *113*, 7756−7764.
63. Perdew, J. P.; Wang, Y. Accurate and Simple Analytic Representation of the Electron-Gas Correlation Energy. *Phys. Rev. B* **1992**, *45*, 13244–13249.